Quenched narrow-line second- and third-stage laser cooling of ^{40}Ca

E. Anne Curtis

National Institute of Standards and Technology, 325 Broadway, Boulder, Colorado 80305, and University of Colorado, Boulder, Colorado 80309

Christopher W. Oates and Leo Hollberg

National Institute of Standards and Technology, 325 Broadway, Boulder, Colorado 80305

Received August 14, 2002; revised manuscript received November 7, 2002

We demonstrate three-dimensional quenched narrow-line laser cooling and trapping of ^{40}Ca. With 5 ms of cooling time we can transfer 28% of the atoms from a magneto-optic trap based on the strong 423-nm cooling line to a trap based on the narrow 657-nm clock transition (which is quenched by an intercombination line at 552 nm), thereby reducing the atoms' temperature from 2 mK to 10 μK. This reduction in temperature should help to reduce the overall systematic frequency uncertainty for our Ca optical frequency standard to <1 Hz. Additional pulsed, quenched, narrow-line third-stage cooling in one dimension yields subrecoil temperatures as low as 300 nK and makes possible the observation of high-contrast two-pulse Ramsey spectroscopic line shapes.

OCIS codes: 140.3320, 300.6320, 300.6360, 020.7010.

1. INTRODUCTION

Alkali atoms are routinely laser cooled to temperatures ranging from 1 to 20 μK (corresponding to several atomic recoils) by the use of optical molasses on strong transitions. In an effort to further reduce atom temperatures, investigators developed new methods to push cooling below the recoil limit that include the use of several new laser-cooling strategies: Raman cooling,[1,2] velocity-selective coherent population trapping,[3,4] and evaporative cooling in dipole traps.[5] Such second-stage cooling schemes have attained temperatures well below 1 μK and have been used in a variety of experimental demonstrations.

Second-stage cooling is particularly important for alkaline-earth elements because magneto-optic traps (MOTs) involving these atoms typically have temperatures of several millikelvins. These relatively high temperatures are the consequence of Doppler-limited cooling on strong transitions that lack the ground-state substructure required for sub-Doppler cooling mechanisms such as polarization-gradient cooling. There is, however, real interest in obtaining colder alkaline-earth atoms, as this would benefit many applications including atom interferometry, quantum degenerate gases, and optical frequency standards. In fact, recent frequency measurements of the Ca clock transition at 657 nm were limited (at $\sim$10 Hz) primarily by residual Doppler effects caused by the millikelvin temperatures of the laser-cooled atoms.[6,7]

In an effort to reduce the temperature of our Ca atoms, we looked to cooling experiments with Sr, whose narrow intercombination line at 689 nm had been used to build a second-stage MOT and achieved submicrokelvin temperatures.[8,9] The corresponding transition in Ca (400-Hz linewidth), although excellent for optical frequency standards, cycles photons too slowly to be used directly useful for second-stage cooling of atomic samples starting with a temperature of several millikelvins. However, by incorporating a technique first demonstrated for sideband cooling with trapped ions,[10] we are able to accelerate the cooling process by *quenching* the excited state, that is, connecting the excited state with another laser to a higher-lying level that decays quickly to the ground state. We previously used quenched narrow-line laser cooling[11] (QNLC) in one dimension to reduce the atomic temperature to 4 μK, thus showing the potential of the technique. For the Ca optical frequency standard, however, full three-dimensional (3-D) cooling is required for reducing the systematic frequency shifts. Quenched cooling and trapping in three dimensions for Ca was first demonstrated at the Physikalisch-Technische Bundesanstalt (PTB), where a quenching transition at 453 nm was used to achieve temperatures of less than 10 μK and transfer efficiencies of $\sim$12%.[12]

Here we describe 3-D second-stage cooling of Ca, in which we use a different quenching transition to achieve similar temperatures but higher transfer efficiency ($\sim$25%). These microkelvin temperatures should enable the Ca optical frequency-standard at 657 nm to achieve a frequency uncertainty of <1 Hz (fractionally $<3 \times 10^{-15}$). Additionally, we use this ultracold sample as a starting point for third-stage QNLC in one dimension; with a stepwise excitation scheme based on our earlier work[11] we can now produce subrecoil temperatures as low as 300 nK for 60% of the ultracold atoms. These submicrokelvin atomic samples derived from our three-stage cooling scheme are then used for what we believe is the first demonstration of two-pulse Ramsey fringes with Ca atoms.

2. THREE-DIMENSIONAL SECOND-STAGE COOLING

A. Experiment

Although the stepwise excitation approach that we used for one-dimensional (1-D) cooling can be extended to three dimensions,[2] it is more straightforward to implement the method demonstrated in Ref. 12 for 3-D cooling and trapping. This approach uses simultaneous rather than sequential excitation of the three-level system (clock + quenching transitions). With the cooling and quenching beams turned on throughout the cooling cycle, the atoms can be continuously cycled and cooled in a manner similar to Doppler cooling between two atomic levels (albeit with a larger net atomic recoil because of the quenching and spontaneous-emission photons). In fact, the three-level QNLC system can be reduced to an equivalent two-level description with an effective transition linewidth equal to the quenching rate. This dependence actually gives quenched cooling an additional (and potentially powerful) degree of freedom, as one can tune the linewidth of the effective Doppler cooling transition simply by changing the quenching power. One can then envisage a cooling procedure that starts with a broad transition linewidth (i.e., with its wide Doppler coverage and fast cooling rate) to cool a large range of velocities and then concludes with reduced quenching power for narrow-line cooling and its associated colder temperatures.

For cooling on the clock transition of Ca, however, it is difficult to achieve high quenching rates because one necessarily must use a weak (intercombination) line to pump atoms from the $^3P_1$ level back to the singlet manifold for quick decay to the ground state. We have chosen to use the $^3P_1 \rightarrow {}^1S_0$ ($4s4p \rightarrow 4s5s$) transition at 552 nm (see Fig. 1) rather than the $^3P_1 \rightarrow {}^1D_2$ ($4s4p \rightarrow 4s4d$) transition at 453 nm used in the research reported in Ref. 12. The two transitions have similar Einstein A coefficients, but the slower (by a factor of 2) decay from the $^1D_2$ state actually accelerates the pumping process, because the pumping rate is proportional to $1/\Gamma$, where Γ is the decay rate of the upper state in the three-level system. However, the advantage of using 453-nm pumping is offset by the fact that the dyes used in the green lasers are generally more powerful and longer lived than those in the blue. In either case, typical quenching times achieved thus far range from 25 to 50 μs, corresponding to cooling linewidths of <10 kHz. These effective cooling linewidths are too narrow for the idealized tunable cooling as described above to be achieved, so we broaden the spectrum of the red laser to extend the capture range of the second-stage cooling light.[8,9,12]

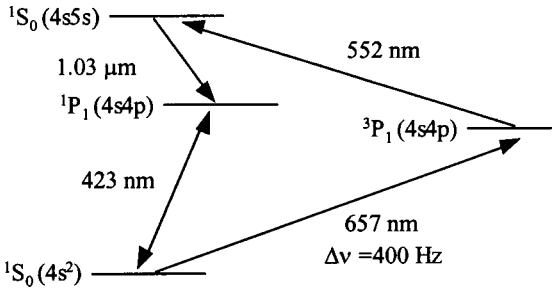

Fig. 1. Energy-level diagram for ^{40}Ca, showing relevant levels for cooling and quenching.

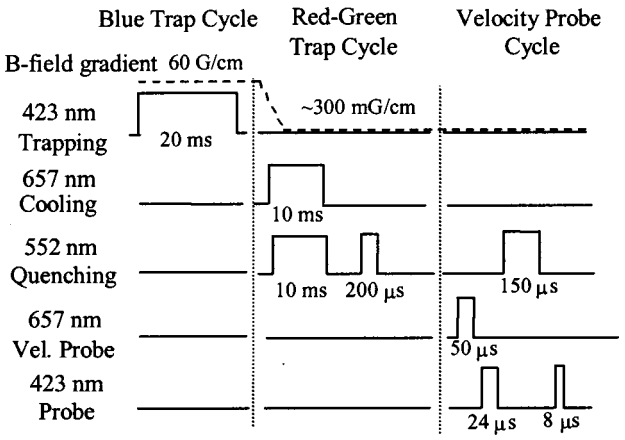

Fig. 2. Timing diagram for second-stage cooling. See text for details of the modified shelving detection scheme.

Our cooling route to microkelvin temperatures (see the timing diagram, Fig. 2) begins with first-stage laser trapping on the strong $^1S_0 \rightarrow {}^1P_1$ transition at 423 nm. The trapping apparatus has been described elsewhere,[13] so we describe only the most relevant details here. A frequency-doubled diode-laser system generates 40 mW of trapping light at 423 nm, which we use to load $\sim 2 \times 10^6$ atoms in 25 ms from an atomic beam into a MOT. The resulting temperature of the trapped atoms is 2–3 mK. We follow this with a cycle of second-stage cooling, which uses simultaneous 657-nm cooling and 552-nm quenching light. The 552-nm light comes from a dye laser whose beam, after passing through an optical fiber and a liquid-crystal light shutter, supplies $\sim$100 mW of light to the atoms. For long-term stability the frequency of the green light is stabilized relative to a hyperfine component of a nearly coincident I_2 transition.

The 657-nm cooling light is generated by an extended-cavity diode laser whose output is amplified by injection locking two slave lasers. The output from one slave passes through a polarization-maintaining fiber and is used for second-stage cooling and trapping. The other slave supplies light to two separate polarization-maintaining fibers that provide counterpropagating beams for spectroscopy and pulsed cooling (see Refs. 11 and 13 for spectroscopic details). Because the red light is used for subkilohertz spectroscopic investigations in addition to the cooling described here, it has extremely high frequency stability. We achieve this stability by locking the laser's frequency tightly to a narrow resonance of a high-finesse Fabry–Perot cavity (linewidth, 9 kHz). The cavity is vibrationally and acoustically isolated, and the addition of temperature stabilization of the box surrounding the cavity has led to drift rates of only a few hertz per second. For cooling, the red light is detuned 850 kHz ($\pm$50 kHz) below resonance and broadened to cover a 1.5-MHz-wide spectrum by application of frequency modulation at 20 kHz to a 72-MHz acousto-optic modulator. Deviations of 20% for these modulation parameters did not noticeably affect the cooling results. This modulation creates a comb of optical frequencies that are close enough together that the atoms remain resonant as they

are cooled. The comb width enables a larger portion of the initial velocity distribution of Ca atoms to be cooled and trapped than with a single frequency alone. The trade-off for this broader spectrum is a less precisely tailored spectrum near zero velocity, so we do not expect to attain the temperatures achievable with single-frequency or pulsed cooling.

The red cooling beams (with an intensity of ~20 mW/cm^2 per beam and a $1/e^2$ diameter of 3 mm) are retroreflected in three orthogonal directions and overlap the blue trapping beams. A single green beam (with an intensity of ~1 W/cm^2 and a $1/e^2$ diameter of 3 mm) has a separate retroreflected path that lies along two orthogonal axes. The polarization of the red beams matches that of the blue trapping beams, which have the usual $\sigma^+ - \sigma^-$ configuration for a MOT. The green beams, however, have the opposite circular polarization to increase the likelihood of absorption of green and red photons from the same direction, thus increasing the cooling force. This increase results from considerations of angular momentum; because the $^1S_0$ upper state of the quenching transition has only an $m = 0$ level, quenching of the $+1$ and -1 levels of the $^3P_1$ state necessarily requires absorption of σ^- and σ^+ light, respectively. To add a spatial (i.e., trapping) component to the narrow-line cooling process we introduced a small magnetic quadrupole field (~30 μT/cm, or ~300 mG/cm), as has been used in similar alkaline-earth MOTs.[8,9,12] The cooling results were not sensitive to the size of the gradient over the range 10–50 μT/cm.

The second-stage cooling is followed by a pulse of quenching light (100–200 μs) that is used to transfer those atoms still residing in the excited state to the ground state for maximum detection efficiency. We then use a red spectroscopic pulse whose frequency is swept to measure the velocity distribution of the atoms along one direction (one point per measurement cycle) by means of the first-order Doppler shift. (Note that this 1-D measurement technique naturally leads us to adopt the usual convention of quoting 1-D values for temperatures and rms velocities regardless of the dimensionality of the cooling.) To prevent broadening, the duration of this pulse is chosen to yield a Fourier-transform width much less than that of the velocity distribution. To take advantage of the presence of the quenching light, we modified the normalized shelving detection scheme (based on near-resonant blue pulses) used in our previous experiments to achieve a high signal-to-noise ratio.[13] Now, instead of using a blue normalization pulse before the spectroscopy, we perform the normalization at the end of the spectroscopic cycle. The detection process begins with a blue probe pulse that occurs after the red velocity probe pulse to measure those atoms left in the ground state (i.e., those not in the velocity class excited by the red probe pulse). Atomic fluorescence excited by the standing-wave blue probe (intensity, ~15 mW/cm^2, with a duration of 20–30 μs) is collected by a lens inside the vacuum system and directed to a photomultiplier tube. The excited atoms are then pumped back to the ground state by a quenching pulse (552 nm, 150-μs duration), and the ground-state population (now equal to the total population of trapped atoms) is measured by a second blue normalization pulse. Dividing the integrated fluorescence of the first pulse by that of the second yields a normalized excitation signal. By keeping the time between intensity-stabilized blue probe pulses short (and thus less sensitive to residual fluctuations in intensity), and by normalizing the excitation signal relative to the number of atoms captured in the red–green trap (rather than to the number in the blue trap), we are able to maintain the signal-to-noise ratio attained in the spectroscopy based on millikelvin atoms. A similar scheme at the PTB recently used a different version of shelving detection with quenching.[14]

As shown in Fig. 3, the temperature of the atom cloud drops rapidly in the first few milliseconds of red–green cooling and then levels off below 9 μK for longer cooling times. The number of atoms transferred from the blue trap to the red–green trap also decreases with trap time (see Fig. 4), as those atoms whose velocity is not within the capture range of the trap (~40 cm/s) rapidly escape the observation region. Similar results were seen for the second-stage MOT used at the PTB but with smaller

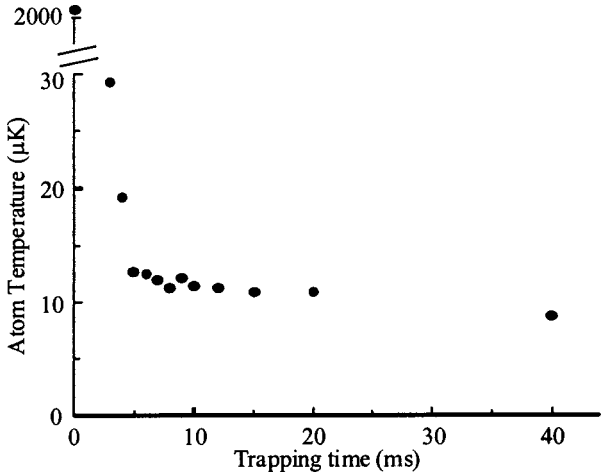

Fig. 3. Temperature of the atom cloud (corresponding to the rms velocity derived from the fit of a Gaussian line shape to the measured velocity distribution) versus second-stage cooling time. Measurements of the velocity distribution in the other two dimensions yield similar results. The initial trap temperature with no second-stage cooling is ~2000 μK.

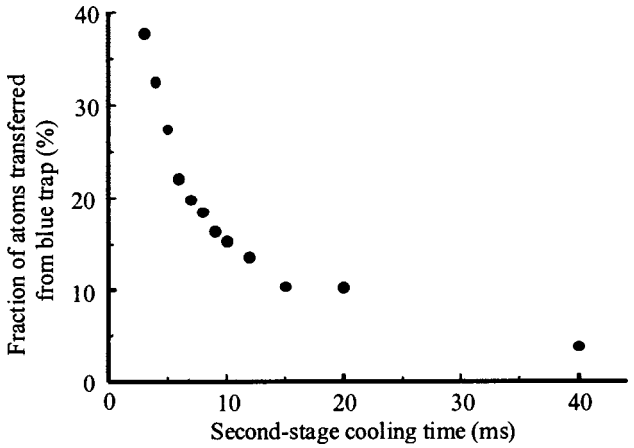

Fig. 4. Fraction of atoms transferred from the blue trap to the red–green trap versus second-stage cooling time.

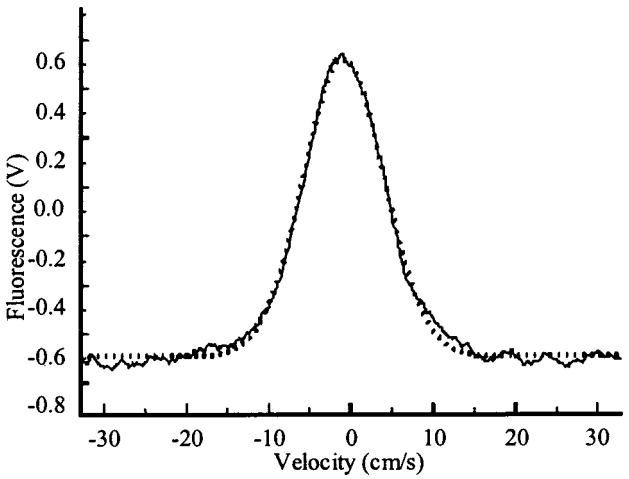

Fig. 5. Atomic velocity distribution after 15 ms of red–green cooling and trapping. A fit to a Gaussian gives a rms velocity of 4.9 cm/s, which corresponds to a temperature of 11.5 μK.

atom-transfer efficiency, which we attribute to less quenching laser power. Figure 5 shows a typical velocity distribution after 15 ms of red–green trapping. The symmetry of the measured final velocity distributions is particularly sensitive to the alignment of the green cooling beam, because an asymmetry of green absorption events leads to an asymmetric force on the atoms. Optimization of the overlap of the retroreflected beams for both the trapping and the quenching light increases the atom number and improves the overall symmetry of the velocity distributions. Although we have not yet fully investigated the dependence of the resultant temperature on all relevant experimental parameters, we suspect that the lowest temperature ($\sim$9 μK) observed for the trapped atoms results from several factors. First, each absorption of a green quenching photon is followed by emission of photons at 1.03 μm and 423 nm, which heats the atomic sample [with an effective recoil of 3 cm/s, corresponding to a temperature of 4.5 μK (Ref. 12)]. Second, because the intensity of the quenching laser determines the effective linewidth of the cooling transition, sufficiently large green power can actually set a lower limit for the temperature. Finally, the resultant velocity distributions can be sensitive to the shape of the cooling light spectrum (determined here by the modulation depth and detuning), as the spectrum contributes to the heating rate of the atoms near zero velocity.

B. Improved Optical Frequency Standard

Our particular motivation for second-stage cooling of Ca is to improve the performance of our optical atomic frequency standard. For this application, an optimized version of this second-stage cooling scheme would ideally have the shortest trapping time (to minimize overall cycle time) and the largest number of atoms (to maximize the signal-to-noise ratio) as well as the coldest temperatures (to attain the highest accuracy). As a compromise, we find that working with a red–green trapping time of 5 ms allows the atom cloud to come into equilibrium (good fit to a Gaussian) at a temperature of 10 μK, with a transfer efficiency of 28% (5.6×10^5 of the originally trapped 2.0×10^6 atoms). With such a narrow distribution, nearly all these atoms contribute to the Bordé–Ramsey interferometry that we use for our clock measurements, and the resultant line shapes are virtually Fourier-transform limited. In Fig. 6 we show a single 100-s scan taken at a resolution of 11.55 kHz with ultracold atoms; the contrast in this Bordé–Ramsey fringe pattern is nearly 40%. We note that the asymmetry in the fringe envelope is real: Computer simulations based on the formalism developed by Bordé *et al.*[15] show the same asymmetric envelope and indicate that it results from atomic recoil shifts. For applications to frequency metrology we actually work at considerably higher resolutions (usually $\sim$1 kHz or less) to have a more sharply defined line center. The inset of Fig. 6 shows the central portion of a fringe pattern with 1.45-kHz resolution.

Let us now consider the improvements that we expect to see in our optical standard based on the parameters we can achieve for our ultracold atomic sample. The most dramatic difference should occur in the overall uncertainty with which we can realize the unperturbed atomic frequency, because we were previously limited by velocity-related frequency shifts. The two main systematic effects related to velocity result from (1) a nonzero transverse drift velocity of the atomic sample combined with a residual mismatch in the overlap of the Bordé–Ramsey spectroscopic beams and (2) moving atoms sampling the phase of probe beams with a finite radius of curvature. Second-stage cooling reduces v_{rms} by a factor of 15, thus reducing the shifts that are due to these effects to $<$1 Hz. In this regime we will be able to evaluate other systematic shifts that were previously overshadowed by velocity-induced effects at well below the hertz level. With all systematic effects taken into account, attainment of a frequency uncertainty of $<$0.4 Hz (corresponding to a fractional uncertainty of $<10^{-15}$) for a Ca standard based on ultracold atoms certainly seems feasible.[14]

A second critical parameter used to characterize clock performance is stability, which is effectively a measure of

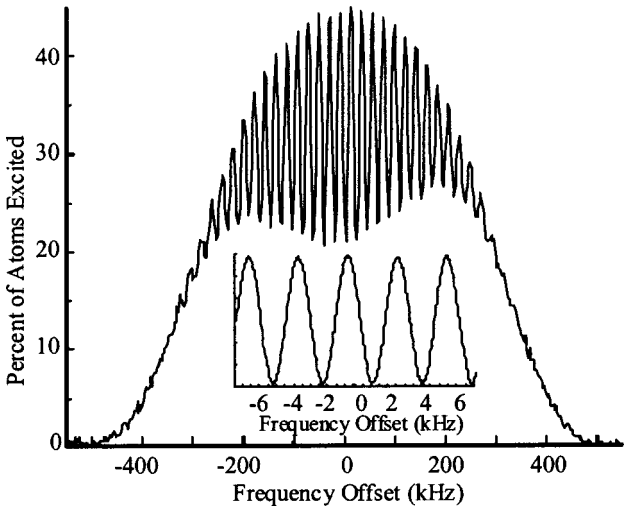

Fig. 6. Bordé–Ramsey fringes based on the $m = 0 \rightarrow m = 0$ levels of the 657-nm clock transition with a resolution of 11.55 kHz taken after 4-ms second-stage cooling. A single 100-s frequency sweep shows high-contrast, Fourier-transform-limited fringes. The asymmetric fringe envelope is a result of atomic recoil. Inset, high-resolution 1.45-kHz Bordé–Ramsey fringes taken under the same cooling conditions ($<$30-s averaging time).

the frequency uncertainty that is achieved for a given averaging time. Because of their high line Q's, optical frequency standards have demonstrated superior short-term stability to that of their microwave counterparts.[16] In Ref. 16, a comparison of our Ca optical clock (based on millikelvin atoms) and a Hg^+ optical clock (based on a single Hg ion) yielded a fractional frequency instability of 7×10^{-15} at 1 s, which represents what is to our knowledge the most stable short-term performance demonstrated with atomic frequency standards. In moving to a clock based on ultracold atoms, we see some trade-offs in terms of short-term stability. The longer loading and preparation time of the atoms leads to a sixfold increase in the duration of the measurement cycle, which will effectively increase the averaging period, degrading short-term stability. Moreover, the number of trapped atoms is reduced by nearly a factor of 10, which also reduces the signal-to-noise ratio. Fortunately, this reduction is mostly offset by the fact that with ultracold atoms basically all the atoms, rather than the ~30% that we had with the millikelvin atoms, contribute to the fringe structure. Accounting for the 2–3-times higher contrast achieved with ultracold atoms at subkilohertz resolutions, we expect to see little net degradation in short-term frequency stability. This expectation is supported by our initial measurements of the fractional frequency instability of the system based on ultracold atoms, which show an Allan deviation of $<2 \times 10^{-14}$ at 1 s. The dominant residual noise appears to be frequency noise on the laser, which we believe results from fluctuations in the length of the optical reference cavity, perhaps aggravated by the Dick effect (for microkelvin atoms our spectroscopic period is only a few percent of the whole measurement cycle).[17,18] The amplitude noise on the detection sets a limit of $<10^{-14}$, so we are confident that with improved cavity isolation and an apparatus better suited for second-stage cooling (with more optical access for capturing more atoms), we should be able to attain a short-term instability of close to 1×10^{-15} at 1 s. We note that even this level of instability is still an order of magnitude worse than estimates of what could be achieved with this Ca transition, so there is still plenty of room for improvement.[14,19]

3. ADDITIONAL ONE-DIMENSIONAL COOLING

A. Experiment

With the capability of starting experiments with trapped atoms at 10 μK rather than at 2 mK, we decided to revisit pulsed QNLC in one dimension.[11] Our previous results had been hindered by two factors associated with the initial millikelvin temperature: The transverse velocity of the atoms sets an upper limit of ~2.5 ms for the cooling time, whereas the width of the velocity distribution required many cooling cycles (i.e., long cooling time) for a majority of the atoms to reach near-zero velocity. With the atoms now starting much closer to zero velocity in three dimensions, we could hope to reach subrecoil temperatures in one dimension for a nontrivial fraction of the atomic sample.

The advantage of using π-pulse excitation on the narrow red transition, followed by a quenching pulse in the green, is that we have greater control over the frequency spectrum of the cooling light. Because the cooling pulses are much shorter than the lifetime of the excited state, the effective excitation spectrum of the light is basically the Fourier transform of the time dependence of the cooling pulse. We use square pulses in the time domain whose frequency is detuned to the red such that the first zero of the resulting $(\sin x/x)^2$ excitation spectrum lies at zero velocity.[1,2,11] This produces an effective dark state near zero velocity in which atoms can accumulate. Because the length of the cooling pulses in time is inversely related to their span in frequency (velocity) space, longer pulses produce a narrower hole near zero velocity and thus colder velocity distributions. The trade-off, however, is that these longer pulses drive a smaller range of velocities toward zero, so it is advantageous to start with a fairly narrow velocity distribution.

A typical three-stage cooling cycle is shown in Fig. 7. We start with our usual blue cooling followed by red–green cooling and add a third stage that consists of a series of cooling pulses that drive the atomic velocities toward the near zero-excitation region near zero velocity. After each pair of sequential red pulses (one from each direction and with an intensity chosen to yield a π-pulse area), a quenching pulse follows that sends the atoms around to the ground state for another cooling cycle. We alternate the directional order of the red pulses from cycle to cycle to enhance the symmetry of the cooling process. To use the $m = 0 \rightarrow m = 0$ magnetic-field-insensitive transition for this third-stage cooling, we use linearly polarized red light along with a magnetic bias field of 200 μT along the same direction. The red cooling pulses are derived from the same laser and optical fibers that generate the spectroscopic pulses. To tailor the pulses, we use switches to send different rf signals to the acousto-optic modulators that are controlling the intensity and frequency of the red light. Note that we use the same quenching polarization and spatial configuration as in the second stage, which in our present beam geometry means that green light propagates both perpendicularly and parallel to the pulsed red light. As a result of the quenching

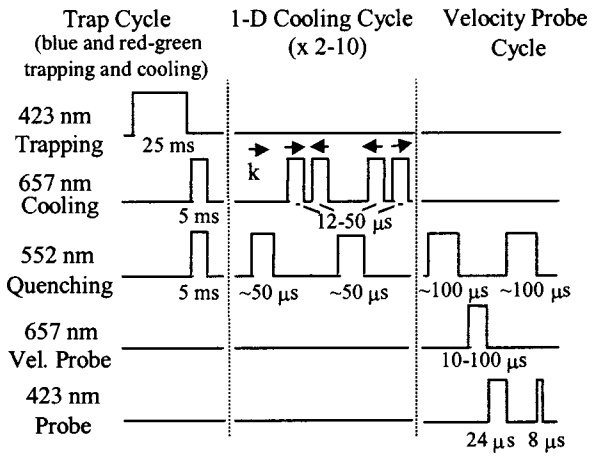

Fig. 7. Timing diagram for three-stage cooling showing the additional 1-D narrow-line quenched cooling.

process, the atoms experience several recoils as they are pumped back to the ground state. Those atoms whose resultant velocity falls near zero will likely avoid reexcitation, whereas the remaining atoms will undergo another cooling cycle. This process repeats until the atoms have all fallen into the near-zero-velocity dark state or by virtue of an unfavorable recoil sequence have landed outside the velocity range covered by the excitation pulses. As before, we use high-resolution 657-nm velocity probe pulses to measure the final width of the velocity distribution along the direction of the 1-D cooling pulses.

In Fig. 8 we show the 1-D velocity distribution that results from a series of eight cycles of third-stage cooling with pulses of 10-μs duration. Each cycle contains a quenched red sequence followed by a quenched red sequence with the pulses in opposite order; see Fig. 7. Note that we find that, for cooling with pulses of duration <15 μs, the velocity distributions fit Lorentzian line shapes rather than Gaussians, as was the case for 3-D cooling, so

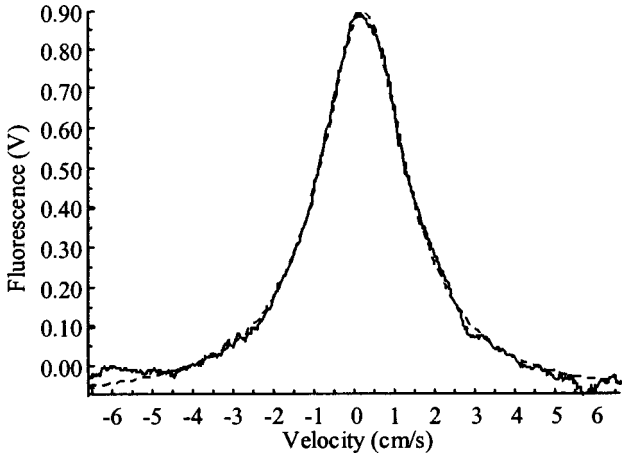

Fig. 8. Velocity distribution after 6-ms second-stage cooling followed by eight cycles of 1-D single-frequency 15-μs red pulses and green quenching. A fit to a Lorentzian yields a velocity (HWHM) of 1.31 cm/s (subrecoil), which corresponds to a temperature of 840 nK.

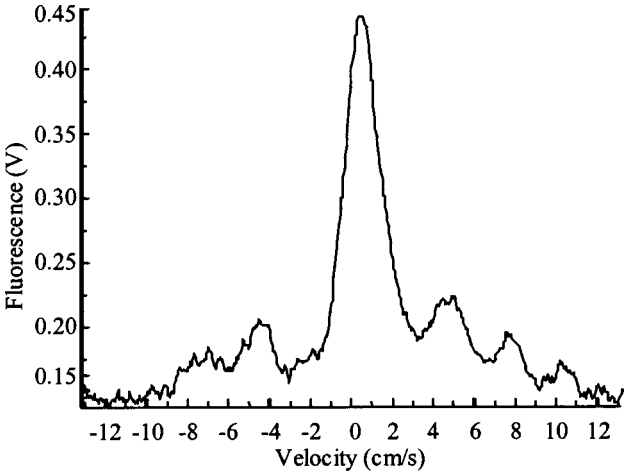

Fig. 9. Velocity distribution after 5-ms second-stage cooling followed by five cycles of 15-μs pulses and eight cycles of 25 μs pulses of red–green cooling. A fit of the narrow central feature to a Lorentzian yields a velocity (HWHM) of 1.0 cm/s (two-thirds of a recoil) and a temperature of 520 nK.

the 1-D results are quoted for the half-width at half-maximum (HWHM) of the Lorentzian instead of a rms width.[20] For a sequence of eight cycles the resultant V_{HWHM} of the distribution is 1.3 cm/s (corresponding to a temperature of 840 nK), approximately equal to the recoil limit (for a single 657-nm photon). Interestingly, a majority of the cooling occurs during the first two cycles, during which minimal heating of the transverse directions should occur.

As we increase the length of the pulses beyond 15 μs to reach lower temperatures, additional structure begins to appear in the baseline of the velocity distributions as more atoms gain access to $(\sin x/x)^2$ zeros that are not centered at zero velocity. These additional dark states limit the transfer efficiency into the coldest central peak (similar structure was seen in our original QNLC experiments). To reduce this effect we implement sequences that use pulses of different lengths (each with its associated detuning). In one case we make the first pulse short such that it transfers a large number of atoms toward zero velocity and make the second pulse long such that it produces a narrow velocity distribution. A sequence consisting of five cycles of 15-μs pulses followed by eight cycles of 25-μs pulses leads to a central feature with a temperature of $\sim$520 nK (see Fig. 9). One can see here the atoms accumulating in small peaks surrounding the other zeros of the $(\sin x/x)^2$ function. We find that, under these conditions, if we allow the atoms to decay directly from the excited state to avoid the recoils associated with quenching, fewer atoms escape the capture region. Waiting for the atoms to decay naturally has, however, the undesirable property of increasing the cooling time by a factor of 4. In an effort to achieve colder temperatures while maintaining good transfer efficiency, we employ a sequence of five cooling cycles with 15-μs pulses followed by five cycles with 50-μs pulses. For the last five cooling cycles the quenching pulses are not used; instead the atoms are allowed to decay naturally over a period of 300 μs. This combination produces a velocity distribution whose central narrow feature has a temperature of only 300 nK (one fourth of the single 657-nm photon recoil temperature) and transfers $\sim$50% of the atoms to the central peak.

B. Spectroscopy

In preliminary experiments the third-stage 1-D cooling did not lead to a marked improvement in the fringe contrast for four-pulse Bordé-Ramsey spectroscopy, as we were already close to the theoretical limit of 50% contrast. However, this extra cooling stage does reduce the velocity of the atoms to the point where the atoms move only a small fraction of an optical wavelength for times as long as 20 μs. In this case we can obtain Ramsey fringe structure by using only two pulses, as in the case of microwave Ramsey spectroscopy. Figure 10 shows two-pulse fringes for a Ramsey time (time between red pulses) of 5 μs. For longer times the fringe contrast degrades as the atoms move a greater fraction of a wavelength, thus adding a spatial component to the interference process that effectively washes out the fringes. Nonetheless, with subrecoil temperatures we can observe fringes for Ramsey times beyond 20 μs. Not surprisingly, the fringe contrast

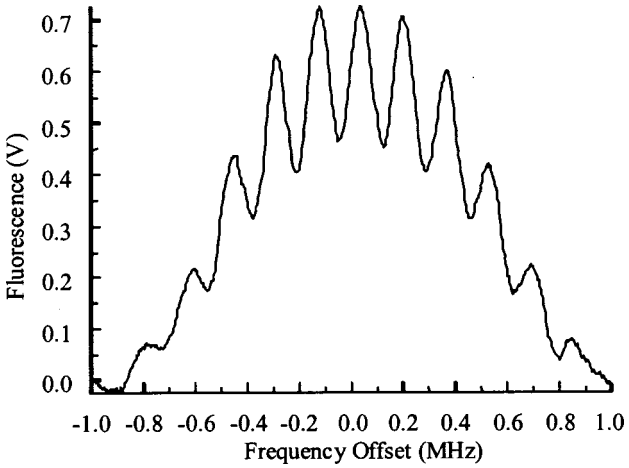

Fig. 10. Two-pulse Ramsey fringes with 1-μs red pulses separated by a 5-μs Ramsey time. Fourier-transform-limited spectrum.

is highly sensitive to velocity; computer simulations of this process yield velocity widths in good agreement with our direct measurements of the velocity distributions. Because of their first-order Doppler sensitivity and reduced contrast at high resolution, these two-pulse fringes will not supersede the four-pulse variety for our immediate frequency-standard applications, but they do offer a nice demonstration of the increased coherence of the atomic sample. Whereas this is the first demonstration of two-pulse fringes in Ca, we emphasize that two-pulse fringes were previously seen in the analogous transition in ultracold Sr.[20]

4. CONCLUSIONS

We have demonstrated three-dimensional second-stage laser cooling and trapping of Ca with fairly high transfer efficiency. Ca atoms at microkelvin temperatures will greatly reduce the dominant systematic frequency shifts for the Ca optical frequency standard but will also serve as a good starting place for further experiments. We showed one example in which we used pulsed cooling in one dimension to reduce the temperature below the recoil limit. Other possible starting points include ramping up the magnetic field gradient to increase the density in preparation for further cooling toward Bose–Einstein condensation.[21] As has been demonstrated with Sr,[22] these ultracold traps can serve as a good starting place for loading far-detuned optical lattices. In fact, a promising approach to an optical frequency standard would be to load ultracold atoms into a 1-D optical lattice for sideband cooling on the clock transition and spectroscopic interrogation. Following the work of Katori, one can choose the wavelength for the far-detuned dipole traps such that the Stark shifts for the ground and the excited states would be equal.[23] One could thus perform the spectroscopy on the clock transition with the lattice fields on, mimicking the environment usually associated with trapped ions. Under these conditions one could imagine having virtually a million noninteracting clocks, cooled to the Lamb–Dicke regime, with small systematic uncertainty and frequency instability.

ACKNOWLEDGMENTS

The authors gratefully acknowledge the loan of a dye-laser system by Carl Wieman at the University of Colorado. We thank Richard Fox and Joseph Wells for their critical reading of the manuscript.

E. A. Curtis's e-mail address is curtis@boulder.nist.gov.

REFERENCES

1. M. Kasevich and S. Chu, "Laser cooling below a photon recoil with three-level atoms," Phys. Rev. Lett. **69**, 1741–1744 (1992).
2. J. Reichel, F. Bardou, M. Ben Dahan, E. Peik, S. Rand, C. Salomon, and C. Cohen-Tannoudji, "Raman cooling of cesium below 3 nK: new approach inspired by Lévy flight statistics," Phys. Rev. Lett. **75**, 4575–4578 (1995).
3. A. Aspect, E. Arimondo, R. Kaiser, N. Vansteenkiste, and C. Cohen-Tannoudji, "Laser cooling below the one-photon recoil energy by velocity-selective coherent population trapping," Phys. Rev. Lett. **61**, 826–829 (1988).
4. J. Lawall, F. Bardou, B. Saubamea, K. Shimizu, M. Leduc, A. Aspect, and C. Cohen-Tannoudji, "Two-dimensional subrecoil laser cooling," Phys. Rev. Lett. **73**, 1915–1918 (1994).
5. C. S. Adams, H. J. Lee, N. Davidson, M. Kasevich, and S. Chu, "Evaporative cooling in a crossed dipole trap," Phys. Rev. Lett. **74**, 3577–3580 (1995).
6. T. Udem, S. A. Diddams, K. R. Vogel, C. W. Oates, E. A. Curtis, W. D. Lee, W. M. Itano, R. E. Drullinger, J. C. Bergquist, and L. Hollberg, "Absolute frequency measurements of the Hg^+ and Ca optical clock transitions with a femtosecond laser," Phys. Rev. Lett. **86**, 4996–4999 (2000).
7. G. Wilpers, "Ein optisches Frequenznormal mit kalten und ultakalten Atomen," Ph.D. dissertation (University of Hannover, Hannover, Germany, 2002), p. 85.
8. H. Katori, T. Ido, Y. Isoya, and M. Kuwata-Gonokami, "Magneto-optical trapping and cooling of strontium atoms down to the photon recoil temperature," Phys. Rev. Lett. **82**, 1116–1119 (1999).
9. K. R. Vogel, T. P. Dineen, A. Gallagher, and J. L. Hall, "Narrow-line Doppler cooling of strontium to the recoil limit," IEEE Trans. Instrum. Meas. **48**, 618–621 (1999).
10. F. Diedrich, J. C. Bergquist, W. M. Itano, and D. J. Wineland, "Laser cooling to the zero-point energy of motion," Phys. Rev. Lett. **62**, 403–406 (1989).
11. E. A. Curtis, C. W. Oates, and L. Hollberg, "Quenched narrow-line laser cooling of ^{40}Ca to near the photon recoil limit," Phys. Rev. A **64**, 031403(R) (2001).
12. T. Binnewies, G. Wilpers, U. Sterr, F. Riehle, J. Helmcke, T. E. Mehlstäubler, E. M. Rasel, and W. Ertmer, "Doppler cooling and trapping on forbidden transitions," Phys. Rev. Lett. **87**, 123002 (2001).
13. C. W. Oates, F. Bondu, R. Fox, and L. Hollberg, "A diode-laser optical frequency standard based on laser-cooled Ca atoms: sub-kilohertz spectroscopy by optical shelving detection," Eur. J. Phys. **7**, 449–460 (1999).
14. G. Wilpers, T. Binnewies, C. Degenhardt, U. Sterr, J. Helmcke, and F. Riehle, "An optical clock with ultracold neutral atoms," Phys. Rev. Lett. **89**, 230801 (2002).
15. Ch. J. Bordé, Ch. Salomon, S. Avrillier, A. Van Lerberghe, Ch. Bréant, D. Bassi, and G. Scoles, "Optical Ramsey fringes with traveling waves," Phys. Rev. A **30**, 1836–1848 (1984).
16. S. A. Diddams, T. Udem, K. R. Vogel, C. W. Oates, E. A. Curtis, W. D. Lee, W. M. Itano, R. E. Drullinger, J. C. Bergquist, and L. Hollberg, "An optical clock based on a single trapped $^{199}Hg^+$ ion," Science **293**, 825–828 (2001).
17. G. J. Dick, "Local oscillator induced instabilities in trapped ion frequency standards," in *Proceedings of the 19th Annual Precise Time and Time Interval (PTTI) Applications and Planning Meeting, Redondo Beach, California, December*

1–3, 1987 (U.S. Naval Observatory, Washington, D.C., 1988), pp. 133–147.
18. L. Maleki, ed., special issue on the Dick effect, IEEE Trans. Ultrason. Ferroelectr. Freq. Control **45**, 876–905 (1998).
19. L. Hollberg, C. W. Oates, E. A. Curtis, E. N. Ivanov, S. A. Diddams, Th. Udem, H. G. Robinson, J. C. Bergquist, W. M. Itano, R. E. Drullinger, and D. J. Wineland, "Optical frequency standards and measurements," IEEE J. Quantum Electron. **37**, 1502–1513 (2001).
20. Lorentzian line shapes were also observed for ultracold Sr atoms, as reported by K. R. Vogel, "Laser cooling on a narrow atomic transition and measurement of the two-body cold collision loss rate in a strontium magneto-optical trap," Ph.D. dissertation (University of Colorado, Boulder, Colo., 1999), pp. 159–183.
21. M. H. Anderson, J. R. Ensher, M. R. Matthews, C. E. Wieman, and E. A. Cornell, "Observation of Bose–Einstein condensation in a dilute atomic vapor," Science **269**, 198–201 (1995).
22. H. Katori, T. Ido, and M. Kuwata-Gonokami, "Optimal design of dipole potentials for efficient loading of Sr atoms," J. Phys. Soc. Jpn. **68**, 2479–2482 (1999).
23. H. Katori, "Spectroscopy of strontium atoms in the Lamb–Dicke confinement," in *Proceedings of the Sixth Symposium of Frequency Standards and Metrology*, P. Gill, ed. (World Scientific, Singapore, 2001), pp. 323–330.